JOURNAL OF SOLID STATE CHEMISTRY 105, 151–160 (1993)

Raman Spectroscopic Studies of $Y_2(SO_4)_3$ Substitution in $LiNaSO_4$ and $LiKSO_4$

ROGER FRECH

Department of Chemistry and Biochemistry, University of Oklahoma, Norman, Oklahoma 73019

RENEE COLE

Department of Chemistry, Hendrix College, Conway, Arkansas 72032

AND GAMINI DHARMASENA

Department of Chemistry and Biochemistry, University of Oklahoma, Norman, Oklahoma 73019

Received August 31, 1992; in revised form November 30, 1992; accepted December 2, 1992

Lithium sodium sulfate, $LiNaSO_4$, and lithium potassium sulfate, $LiKSO_4$, have been prepared with yttrium sulfate, $Y_2(SO_4)_3$, as a substituent over a concentration range up to 15 mol%. Raman spectra of the sulfate ion intramolecular modes suggest the formation of a new compound in the substituted materials. The possibility of substitutional stabilization of a higher temperature phase in the parent compounds is ruled out by comparison with the spectrum of the high temperature phase in each pure parent compound. A differential scanning calorimetry study of substituted $LiKSO_4$ shows an endothermic process at 281°C not present in the pure compound. Powder X-ray diffractograms of the substituted $LiKSO_4$ compounds indicate the presence of pure $LiKSO_4$, pure $Y_2(SO_4)_3$, and new peaks not attributable to either component.

Introduction

One of the more recently studied examples of phase stabilization occurs in aliovalently substituted sodium sulfate Na_2SO_4, which is a highly polymorphic material although there is some disagreement as to the number of phases and the temperature range of those phases (*1–6*). Phase I, which is the thermodynamically stable phase from 237°C to the melting point at 883°C, is of particular interest since it exhibits a high degree of ionic conductivity, e.g., $\sigma = 1.1 \times 10^{-5}$ S cm^{-1} at 250°C (*7*). Although this phase is described by a bimolecular unit cell in the hexagonal space group $P6_3/mmc$ (*8*), the basic structure of Na_2SO_4(I) has also been the subject of conflicting reports in the literature (*9–11*). It has been recognized for some time that up to 30% cation vacancies can be formed in phase I of sodium sulfate by aliovalent cation substitution (*12*). What is especially noteworthy is that in some cases aliovalent substitution stabilizes the high temperature phase I down to room temperature, in other words phase stabilization occurs over a range of 200°C. This effect can be rather dramatic; for example, phase I can be stabilized at room temperature by as little as 1.2 mole% $Y_2(SO_4)_3$ (*8*). Therefore we decided to examine the effect of aliovalent cation substitution in analogous sulfate-containing crystals, specifically lithium sodium sulfate and lithium potassium sulfate.

Lithium sodium sulfate, $LiNaSO_4$, crystallizes in the $P31c$ (C_{3v}^4) space group with

0022-4596/93 $5.00

six molecular units in the hexagonal cell (*13*). The irreducible representations of the internal optic modes are $\Gamma = 9A_1 + 9A_2 + 18E$ and originate in the intramolecular vibrations of the sulfate ion. At 518°C this compound undergoes a phase transition into the body-centered cubic phase (*14*) which has high ionic conductivity (*15*).

Lithium potassium sulfate, $LiKSO_4$, forms a bimolecular unit cell in the $P6_3$ (C_6^6) space group (*16*). The irreducible representations of the sulfate ion internal modes are $\Gamma = 3A + 3B + 3E_1 + 3E_2$. A transition into an orthorhombic phase occurs at 436°C (*17*) although no phase of this compound is reported to exhibit unusually high ionic conductivity.

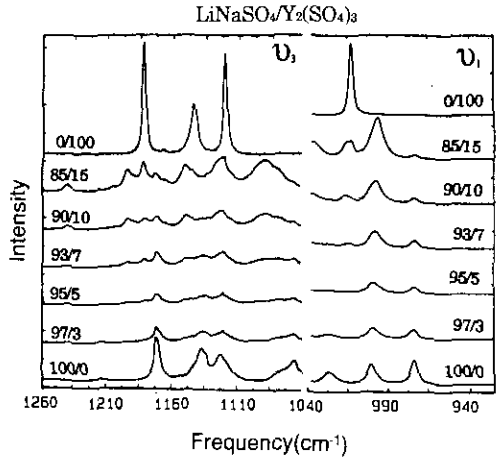

FIG. 1. Raman scattering spectra of $LiNaSO_4$ substituted with $Y_2(SO_4)_3$ in the ν_3 and ν_1 sulfate ion intramolecular mode spectral regions. The relative concentrations in mole% ratios are indicated on each spectrum.

Experimental

Single crystals of each compound were grown by slow evaporation from aqueous solutions, with details of the solution preparation and growth temperatures described elsewhere (*18, 19*). The yttrium sulfate-substituted materials were prepared by melting appropriate amounts of the host salt with $Y_2(SO_4)_3$ (prepared from $Y_2(SO_4)_3 \cdot H_2O$, 99.9% purity, AESAR) at 950°C for 6 hr, lowering the temperature to 700°C for 3 hr, and then cooling to room temperature over a period of approximately 6 hr. The resulting polycrystalline mass was ground to a powder with a mortar and pestle and packed into a capillary tube for spectral studies. Raman spectra were recorded at a 3-cm^{-1} spectral slitwidth on a system based on a 0.85-m Czerny-Turner double monochromator. The 488.0 nm line of an argon-ion laser was used for excitation at 400 mW output power. The spectrometer was calibrated using a neon lamp and the standard reference values of neon emission lines in air.

Experimental Results

Lithium Sodium Sulfate

In the ν_1 spectral region of pure $LiNaSO_4$ the three modes at 1027, 1000, and 973 cm^{-1} as previously reported (*19*) are easily seen in Fig. 1. These are observed in all compositions, although with successive $Y_2(SO_4)_3$ doping, the intensity of the middle component grows relative to the other two. In the .93/.07 system a feature at 1013 cm^{-1} can be observed which is identified as belonging to $Y_2(SO_4)_3$ by comparison with the upper spectrum. However, an additional band at 1036 cm^{-1} is seen in the .90/.10 system which does not belong to either the host or dopant compounds. The intensity of this feature increases with intensity and appears to signal the appearance of a new compound or phase.

Components of the ν_3 vibrational multiplet are seen in pure $LiNaSO_4$ and the substituted compounds in Fig. 1 at 1174, 1139, 1124, and 1070 cm^{-1}. In the spectrum of the .90/.10 composition the most intense component of the pure $Y_2(SO_4)_3$ can be seen at 1184 cm^{-1} with other bands at 1145 and 1122 cm^{-1}. However, five new components are observed at 1241, 1195, 1174, 1151, and 1092 cm^{-1}. The latter band is broad and appears to have some underlying structure. It would first appear that the new mode at 1151 cm^{-1} corresponds to the pure $Y_2(SO_4)_3$ mode at 1145 cm^{-1}. However, the exact coincidence

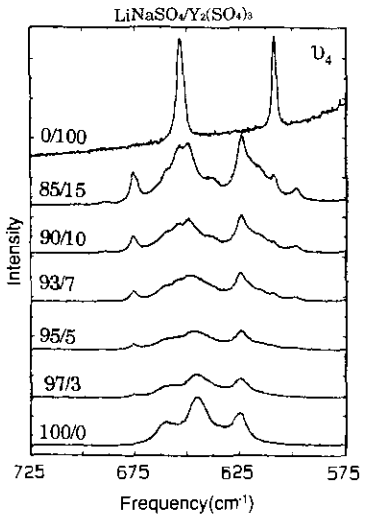

FIG. 2. Raman scattering spectra of $LiNaSO_4$ substituted with $Y_2(SO_4)_3$ in the ν_4 sulfate ion intramolecular mode spectral region. The relative concentrations in mole% ratios are indicated on each spectrum.

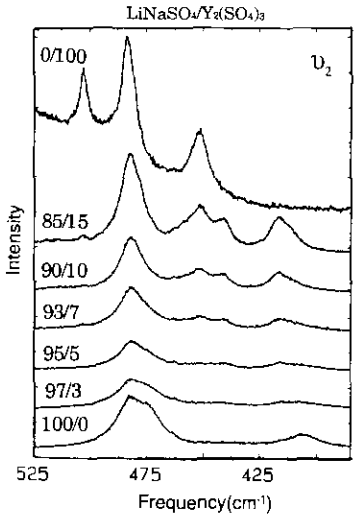

FIG. 3. Raman scattering spectra of $LiNaSO_4$ substituted with $Y_2(SO_4)_3$ in the ν_2 sulfate ion intramolecular mode spectral region. The relative concentrations in mole% ratios are indicated on each spectrum.

of all other modes attributable to the appearance of the pure $Y_2(SO_4)_3$ phase argues against this identification; further, both modes can be seen in the .85/.15 sample (not shown).

The ν_4 region shows similar behavior as is evident in Fig. 2. The $LiNaSO_4$ bands at 661, 646, and 625 cm^{-1} are observed in all compositions while the two $Y_2(SO_4)_3$ components at 654 and 609 cm^{-1} can be seen growing in the more highly doped compositions. New bands which increase in intensity with increasing dopant concentration are seen at 676, 650, 638, and 599 cm^{-1}. In addition there is an intensity increase in the low frequency wing of the 625 cm^{-1} band.

The ν_2 region is somewhat complicated because of the near coincidence of the Li $NaSO_4$ band at 482 cm^{-1} and the $Y_2(SO_4)_3$ band at 484 cm^{-1} as noted in Fig. 3. Two additional $Y_2(SO_4)_3$ components at 501 and 452 cm^{-1} are observed to grow with increasing concentration; however, a new feature at 441 cm^{-1} is also seen. The band at 406 cm^{-1} in pure $LiNaSO_4$ has been previously identified through lithium isotopic substitution studies as a lithium mode, and the new mode appearing at 417 cm^{-1} in the more highly doped samples may be an analogous feature.

In each spectral region the data provide a consistent picture. Between 3 and 5 mole%

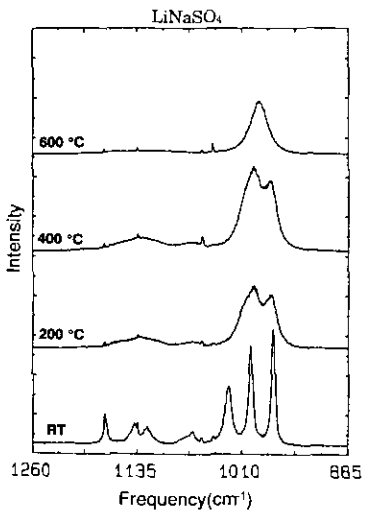

FIG. 4. Raman scattering spectra of pure $LiNaSO_4$ in the ν_3 and ν_1 sulfate ion intramolecular mode spectral regions as a function of temperature. The spectrum at 600°C corresponds to the high temperature phase.

TABLE I

FREQUENCIES (IN cm^{-1}) OF THE SULFATE ION INTRAMOLECULAR MODES IN $Y_2(SO_4)_3$-SUBSTITUTED $LiNaSO_4$

Spectral region	$LiNaSO_4$	New compound	$Y_2(SO_4)_3$	$LiNaSO_4$ (α phase)
ν_1	1027	1036	1013	991
	1000			
	973			
ν_2	482	441	484	456
			452	
			501	
ν_3	1174	1241	1184	1110
	1139	1195	1145	
	1124	1174	1122	
	1070	1151		
		1092		
ν_4	661	676	654	629
	646	650	609	
	625	638		
		599		

Note. The first three columns list the frequencies which can be attributed to the pure room temperature phase $LiNaSO_4$, the new compound, and phase-separated $Y_2(SO_4)_3$. For comparison the last column lists the sulfate ion frequencies in the high temperature α phase of $LiNaSO_4$.

$Y_2(SO_4)_3$ substitution, bands appear which signal the appearance of a new phase or compound. In roughly this same concentration range, additional bands appear which can be unambiguously identified as bulk $Y_2(SO_4)_3$. The question is whether the new bands are due to the stabilized high temperature phase. This can be checked by examining the Raman spectrum of pure $LiNaSO_4$ above the phase transition temperature. The

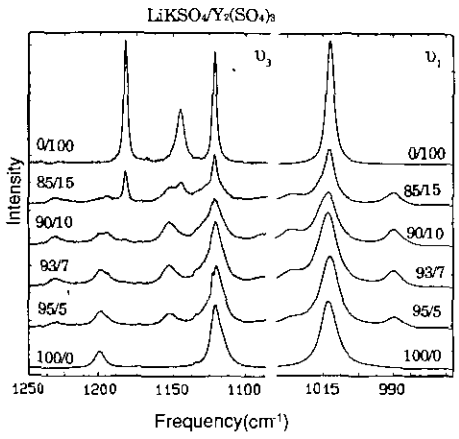

FIG. 5. Raman scattering spectra of $LiKSO_4$ substituted with $Y_2(SO_4)_3$ in the ν_3 and ν_1 sulfate ion intramolecular mode spectral regions. The relative concentrations in mole% ratios are indicated on each spectrum.

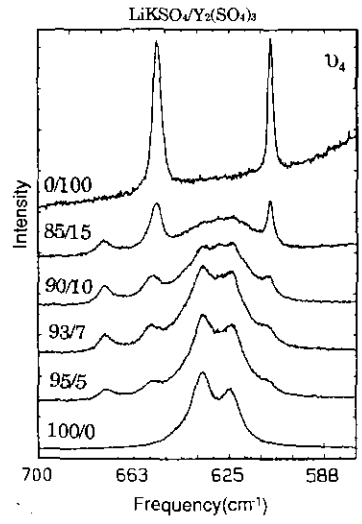

FIG. 6. Raman scattering spectra of $LiKSO_4$ substituted with $Y_2(SO_4)_3$ in the ν_4 sulfate ion intramolecular mode spectral region. The relative concentrations in mole% ratios are indicated on each spectrum.

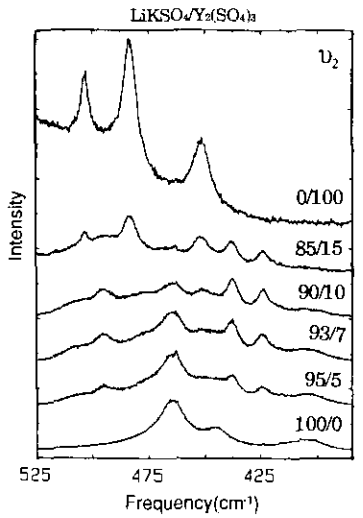

FIG. 7. Raman scattering spectra of $LiKSO_4$ substituted with $Y_2(SO_4)_3$ in the ν_2 sulfate ion intramolecular mode spectral region. The relative concentrations in mole% ratios are indicated on each spectrum.

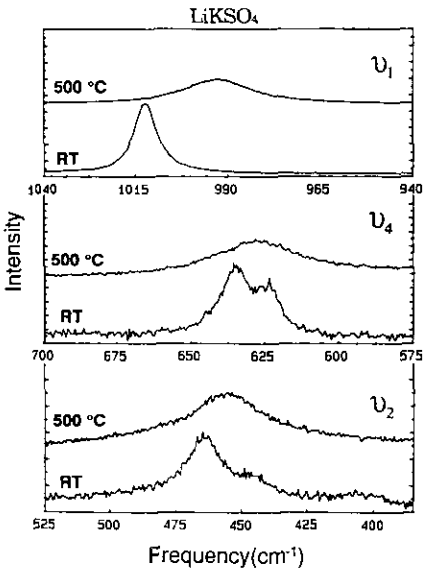

FIG. 8. Raman scattering spectra of pure $LiKSO_4$ in the ν_1, ν_4, and ν_2 sulfate ion intramolecular mode spectral regions as a function of temperature. The spectra at 500°C correspond to the high temperature phase.

temperature dependence of the ν_1 and ν_3 spectral region is illustrated in Fig. 4. In the high temperature cubic phase (600°C spectrum) there is a single ν_1 band at 991 cm^{-1}. This clearly does not correspond to the new band in the substituted spectrum at 1036 cm^{-1}. Above the phase transition only a very weak and broad band centered at roughly 1110 cm^{-1} is observable in the ν_3 region. This also does not coincide with any of the components in the substituted system.

The temperature dependence of the ν_1 vibrational multiplet is quite interesting. The

TABLE II

FREQUENCIES (cm^{-1}) OF THE SULFATE ION INTRAMOLECULAR MODES IN $Y_2(SO_4)_3$-SUBSTITUTED $LiKSO_4$

Spectral region	$LiKSO_4$	New compound	$Y_2(SO_4)_3$	$LiKSO_4$ (high T)
ν_1	1013	1026	1013	995
		990		
ν_2	465	495	504	457
	445	438	484	
	405	424	452	
ν_3	1201	1232	1184	1100
	1121	1198	1145	
		1153	1122	
ν_4	636	675	654	628
	625		609	

Note. The first three columns list the frequencies which can be attributed to the pure room temperature phase $LiKSO_4$, the new compound, and phase-separated $Y_2(SO_4)_3$. For comparison the last column lists the sulfate ion frequencies in the high temperature phase of $LiKSO_4$.

TABLE III

VALUES OF 2θ, d-SPACINGS, AND RELATIVE INTENSITIES OF PURE $LiKSO_4$, $Y_2(SO_4)_3$-SUBSTITUTED $LiKSO_4$ AT A MOLAR RATIO OF 10:90, AND PURE $Y_2(SO_4)_3$

$LiKSO_4$			$LiKSO_4/Y_2(SO_4)_3$			$Y_2(SO_4)_3$		
2θ	d(Å)	I(rel)	2θ	d(Å)	I(rel)	2θ	d(Å)	I(rel)
			11.85	7.462	5.4			
			12.00	7.369	9.7			
			12.20	7.249	7.1			
			12.90	6.857	6.1			
			13.20	6.702	9.4			
						14.00	6.320	12.6
			14.30	6.188	27.6			
			14.90	5.941	35.5			
			17.70	5.007	14.1			
			18.80	4.716	6.4			
20.70	4.287	19.5	20.70	4.287	9.8			
			20.90	4.247	7.9			
			22.15	4.010	17.7			
22.50	3.948	19.3	22.55	3.940	93.5	22.60	3.931	5.7
			24.65	3.609	14.5			
			25.00	3.559	41.9			
			26.40	3.373	5.1			
			26.70	3.336	10.3			
			27.15	3.282	17.4			
			28.25	3.156	13.1			
28.85	3.092	100	28.90	3.087	100			
			29.50	3.025	10.1			
			29.95	2.981	35.5			
						30.25	2.952	100
			30.60	2.919	12.7			
						30.80	2.901	80.2
			31.15	2.869	16.9	31.10	2.873	93.2
			31.40	2.847	13.9			
			32.35	2.765	10.0			
			32.70	2.736	13.9			
35.00	2.562	12.3	35.00	2.562	57.2			
			35.35	2.537	7.1			
			35.55	2.523	8.0			
36.55	2.456	6.5	36.55	2.456	23.2			
37.35	2.406	5.1	37.30	2.409	5.3			
			37.65	2.387	16.3			
			38.10	2.360	5.5			
			38.90	2.313	7.2			
			39.25	2.293	7.9			
			40.15	2.244	7.5	40.30	2.236	3.1
40.55	2.223	1.1	40.60	2.220	6.0			
41.00	2.199	7.1	40.95	2.202	24.0			
			41.40	2.179	12.7			
			41.75	2.162	11.9	41.80	2.159	11.1

highest frequency component quickly collapses while the middle component becomes the most intense of the two remaining components and remains as the only band observable in the high temperature phase. This behavior was previously noted in a single crystal study (*20*). What is particularly interesting is that this temperature-dependent

TABLE III—*Continued*

$LiKSO_4$			$LiKSO_4/Y_2(SO_4)_3$			$Y_2(SO_4)_3$		
2θ	d(Å)	I(rel)	2θ	d(Å)	I(rel)	2θ	d(Å)	I(rel)
41.90	2.154	9.0	41.95	2.152	27.2			
			42.40	2.130	7.0	42.45	2.128	14.9
						42.85	2.109	16.0
						43.70	2.070	20.0
			44.00	2.056	12.0			
						45.25	2.002	25.7
45.90	1.975	3.2	45.90	1.975	10.9			
						46.10	1.967	16.4
			46.60	1.947	6.2			
			46.85	1.938	5.4			
			47.50	1.913	8.3	47.50	1.913	6.1
			47.85	1.699	11.0			
			49.70	1.833	5.1			
			50.00	1.823	9.0	50.10	1.819	4.6
			51.80	1.763	5.1			
52.00	1.757	11.4	52.05	1.756	3.2			
			53.90	1.700	7.7	53.80	1.703	37.0
			54.20	1.691	7.1			
			54.55	1.681	7.4	54.40	1.685	41.5
			54.80	1.674	7.7			
			55.35	1.658	4.2	55.35	1.658	28.4
55.70	1.649	2.8	55.70	1.649	11.3			
			55.90	1.643	7.7			
			56.65	1.623	7.4			
			57.00	1.614	7.4			
57.25	1.608	0.7	57.30	1.607	8.7			
58.90	1.567	3.4	58.95	1.565	13.6			
59.70	1.548	2.5	59.65	1.549	6.4			
			60.20	1.536	6.0			
			62.60	1.483	20.1			
						62.80	1.478	6.8
						64.65	1.441	13.4
						64.90	1.436	8.2
						70.55	1.334	9.0
						70.85	1.329	9.8
						71.85	1.313	5.8
			73.70	1.284	7.3			
						74.60	1.271	9.5
75.75	1.255	1.7	75.80	1.254	8.1			
78.15	1.222	2.8	78.15	1.222	12.9			
						80.65	1.190	7.2
80.95	1.187	4.0	81.00	1.186	9.8	80.95	1.187	3.9
			81.20	1.184	6.8			
						87.00	1.119	5.8
						87.25	1.116	5.7
						87.75	1.111	12.1
						88.05	1.108	9.4
			88.50	1.104	5.1			
						89.05	1.098	6.4
						89.95	1.090	5.4

behavior is similar to behavior which is observed with increasing concentration of $Y_2(SO_4)_3$ as seen in Fig. 1.

In the cubic phase there is only one band at 629 cm^{-1} observed in the ν_4 region and one band at 456 cm^{-1} in the ν_2 region. These spectra are not shown although the frequencies are summarized in Table I. Neither of these bands appears to coincide with any of the corresponding features in the substituted compounds, even allowing for a frequency decrease in high temperature spectra due to thermal effects.

Lithium Potassium Sulfate

It is an interesting coincidence that both $LiKSO_4$ and $Y_2(SO_4)_3$ have a single band in the ν_1 spectral region at 1013 cm^{-1}. With successive $Y_2(SO_4)_3$ doping, two new bands grow in at 990 and 1026 cm^{-1} as noted in Fig. 5.

In the ν_3 spectral region the host bands at 1201 and 1121 cm^{-1} are easily seen at all dopant concentrations as is also evident in Fig. 5. At compositions of .90/.10 and above, the three $Y_2(SO_4)_3$ bands at 1184, 1145, and 1122 cm^{-1} can be observed. However, new features at 1232, 1198, and 1153 cm^{-1} appear between 3 and 5 mole% and increase with dopant concentration.

The ν_4 spectral region is shown in Fig. 6. The two bands of the guest $Y_2(SO_4)_3$ at 654 and 609 cm^{-1} appear at 3% $Y_2(SO_4)_3$ and grow with increasing concentration. The two $LiKSO_4$ bands at 636 and 625 cm^{-1} merge into a broad structured feature in samples containing more than 10% $Y_2(SO_4)_3$. A single new band at 675 cm^{-1} can be observed in the 3% sample and increases with $Y_2(SO_4)_3$ concentration.

Spectra of the ν_2 spectral region are shown in Fig. 7. The host $LiKSO_4$ bands at 465, 445, and 405 cm^{-1} and the dopant $Y_2(SO_4)_3$ bands at 504, 484, and 452 cm^{-1} can be identified in the samples. The appearance of new bands at 495, 438, and 424 cm^{-1} can easily be noted.

Again it is important to address the question of whether the new bands originate in the stabilized higher temperature phase. Figure 8 compares the spectrum of the room temperature hexagonal phase with those of the high temperature orthorhombic phase in the ν_1, ν_4, and ν_2 regions. There is a single ν_1 band at 995 cm^{-1} in the 500°C spectrum which cannot be attributed to the band at 990 cm^{-1} in the substituted compound, since the thermal shift of the band center frequency would tend to place the band at a higher frequency at room temperature. Further, there is no trace of a second component in the high temperature phase. There is only a single band at 628 cm^{-1} in the ν_4 spectral region 500°C which is impossible to identify with the new band at 675 cm^{-1} in the substituted phase. Similarly, the ν_2 spectral region shows a single band at 457 cm^{-1}, which does not coincide with any of the three new components in the substituted material. The spectrum of the ν_3 region (not shown) indicates a very broad, weak feature centered roughly at 1100 cm^{-1}.

The frequencies are summarized in Table II.

Differential Scanning Calorimetry and X-Ray Diffraction Measurements

A thermal analysis was performed on the substituted $LiKSO_4$ compounds using a Perkin-Elmer DSC-2 differential scanning calorimeter. The samples were measured as finely ground powders over a temperature range from 37 to 475°C at a heating rate of 10°/min. An endotherm was observed at 449°C in the pure $LiKSO_4$ compound and was observed to decrease to 444°C at 15 mole% $Y_2(SO_4)_3$. However, an endotherm was observed at 281°C in the 10% substituted compound and continued to increase in relative intensity in the more highly substituted compounds. No corresponding transition was observed in the unsubstituted compound.

Powder X-ray diffraction (XRD) patterns of the substituted $LiKSO_4$ compounds were recorded with a Rigaku DMAX diffractometer using Cu$K\alpha$ radiation (λ = 1.54 Å) monochromated with a graphite crystal. Ta-

ble III shows 2θ values, d-spacings, and relative intensities of the diffraction peaks observed in a sample containing 10 mole% $Y_2(SO_4)_3$ and compares these data with those obtained from similar measurements in pure $LiKSO_4$ and $Y_2(SO_4)_3$. Diffraction peaks of pure $Y_2(SO_4)_3$ and pure $LiKSO_4$ can easily be distinguished in the substituted sample. However, the diffraction pattern appears to be dominated by additional peaks which are not due to either the pure host or the pure guest compound.

Discussion

It is clear from the spectral data of both $LiNaSO_4$ and $LiKSO_4$ that either a new phase or a new compound is formed upon substitution of $Y_2(SO_4)_3$ into the host compound. The appearance of new bands occurs between 3 and 5 mole% of the substituent and is roughly coincident with the appearance of bands originating in phase-separated, pure $Y_2(SO_4)_3$. Comparison of temperature-dependent spectral data of the pure host compounds with the substituted compounds shows that in neither $LiNaSO_4$ nor $LiKSO_4$ can the new bands be attributed to the higher temperature phase which has been stabilized by the presence of $Y_2(SO_4)_3$ as has been previously observed in Na_2SO_4.

The data also argue against vibrational modes originating in sulfate ions of the host lattice locally perturbed by the substituent yttrium ions. The new bands appear with bandwidths which are comparable to the host bands, rather than being very broad with weak scattering intensity as would be expected for bands inhomogeneously broadened by a distribution of potential energy environments in a highly disordered system. Further, the new bands exhibit a vibrational multiplet structure, resembling the factor group components of a compound, particularly in the ν_2, ν_3, and ν_4 spectral regions. In particular, the data in the ν_2 spectral region argue strongly for the formation of a compound. In both substituted Li $NaSO_4$ and $LiKSO_4$ there is a low frequency vibration at 417 cm^{-1} and 424 cm^{-1}, respectively, which may be tentatively assigned to a lithium translatory mode. It is well known from studies of lithium modes in the parent compounds that such modes are highly sensitive to disorder in the local environment (*19*). In the parent compounds the local environment of the lithium ions is defined by the nearest neighbor oxygen atoms of the sulfate ions which tetrahedrally coordinate the lithium ions. With increasing temperature the lithium modes quickly broaden and decrease in scattering intensity, reflecting an increase in the librational amplitude of the sulfate ions. As the librational amplitude increases, the correlated motion of the sulfate ions decreases, and the potential energy environment of the lithium ions becomes increasingly dynamically disordered. Therefore the presence of sharp bands attributed to lithium ion translatory modes in the substituted compounds is a strong argument against any significant local disorder in those materials at the concentrations investigated in this study. Finally, in the case of substituted $LiKSO_4$, both the differential scanning calorimetry and the powder X-ray diffraction data clearly argue for the formation of a new compound.

Acknowledgments

We gratefully acknowledge the help of Professor Barry Weaver, School of Geology and Geophysics, for allowing us access to the powder X-ray diffractometer. We also thank Dr. Bing-Man Fung for allowing us to use the differential scanning calorimeter in his laboratory. One of us (RC) acknowledges financial support from the National Science Foundation REU program.

References

1. F. C. KRACEK, *J. Phys. Chem.* **33,** 1281 (1921).
2. F. C. KRACEK AND C. J. KSANDA, *J. Phys. Chem.* **34,** 1741 (1930).
3. H. F. FISCHMEISTER, *Acta Crystallogr.* **7,** 776 (1954).
4. G. E. BRODALE AND W. F. GIAUQUE, *J. Phys. Chem.* **76,** 737 (1972).
5. C. A. CODY, L. DICARLO, AND R. K. DARLINGTON, *J. Inorg. Nucl. Chem.* **43,** 398 (1981).

6. F. EL-KABBANY, Y. BADR, AND T. TOSSON, *Phys. Status Solidi A* **63,** 699 (1981).
7. M. A. CAREEM AND B. E. MELLANDER, *Solid State Ionics* **15,** 327 (1985).
8. W. EYSEL, H. H. HOFER, K. L. KEESTER, AND TH. HAHN, *Acta Crystallogr. Sect. B* **41,** 5 (1985).
9. M. A. BREDIG, *J. Phys. Chem.* **47,** 587 (1943).
10. K. KOBAYASHI AND Y. SAITO, *Thermochim. Acta* **53,** 299 (1982).
11. H. H. HOFER, Ph. D. dissertation, Technische Hochschule Aachen, Federal Republic of Germany (1979).
12. K. L. KEESTER, W. EYSEL, AND TH. HAHN, *Acta Crystallogr. Sect. A* **31,** 579 (1975).
13. B. MORISON AND D. L. SMITH, *Acta Crystallogr.* **22,** 906 (1967).
14. K. SCHROEDER AND A. KVIST, *Z. Naturforsch. A* **23,** 773 (1968).
15. A.-M. JOSEFSON AND A. KVIST, *Z. Naturforsch. A* **24,** 466 (1969)
16. A. J. BRADLEY, *Philos Mag.* **49,** 1225 (1925).
17. K. SCHROEDER, Ph.D. thesis, University of Gothenburg, Göteborg, Sweden (1975).
18. D. TEETERS AND R. FRECH, *J. Chem. Phys.* **76,** 799 (1982).
19. D. TEETERS AND R. FRECH, *Phys. Rev. B* **26,** 4132 (1982).
20. R. FRECH AND D. TEETERS, *J. Phys. Chem.* **88,** 417 (1984).